



Published in final edited form as:

Leukemia. 2021 November ; 35(11): 3139–3151. doi:10.1038/s41375-021-01219-z.

CCR5 maintains macrophages in the bone marrow and drives hematopoietic failure in a mouse model of severe aplastic anemia

Allison N. Seyfried¹, Amanda McCabe^{1,3}, Julianne N. P. Smith^{1,4}, Laura M. Calvi², Katherine C. MacNamara¹

¹Department of Immunology and Microbiology, Albany Medical College, Albany, NY, USA

²Department of Medicine, Wilmot Cancer Institute, University of Rochester Medical Center, Rochester, NY, USA

³Present address: Boston Children's Hospital TransLab, Translational Research Program, Boston, MA, USA

⁴Present address: Department of Medicine, Case Western Reserve University, Cleveland, OH, USA

Abstract

Severe aplastic anemia (SAA) is an acquired, T cell-driven bone marrow (BM) failure disease characterized by elevated interferon gamma (IFN γ), loss of hematopoietic stem cells (HSCs), and altered BM microenvironment, including dysfunctional macrophages (M Φ s). T lymphocytes are therapeutic targets for treating SAA, however, the underlying mechanisms driving SAA development and how innate immune cells contribute to disease remain poorly understood. In a murine model of SAA, increased beta-chemokines correlated with disease and were partially dependent on IFN γ . IFN γ was required for increased expression of the chemokine receptor CCR5 on M Φ s. CCR5 antagonism in murine SAA improved survival, correlating with increased platelets and significantly increased platelet-biased CD41^{hi} HSCs. T cells are key drivers of disease, however, T cell-specific CCR5 expression and T cell-derived CCL5 were not necessary for disease. CCR5 antagonism reduced BM M Φ s and diminished their expression of *Tnf* and *Ccl5*, correlating with reduced frequencies of IFN γ -secreting BM T cells. Mechanistically, CCR5 was intrinsically required for maintaining BM M Φ s during SAA. *Ccr5* expression was significantly increased in M Φ s from aged mice and humans, relative to young counterparts. Our data identify CCR5 signaling as a key axis promoting the development of IFN γ -dependent BM failure, particularly relevant in aging where *Ccr5* expression is elevated.

[✉]Katherine C. MacNamara, macnamk@amc.edu.

Author contributions ANS designed and performed experiments, analyzed data, and wrote the paper, AM and JNPS designed and performed experiments, and analyzed data, LMC designed experiments and analyzed data, and KCM conceived of the project, designed experiments, analyzed data, and wrote the paper.

Compliance with ethical standards

Conflict of interest The authors declare no competing interests.

Supplementary information The online version contains supplementary material available at <https://doi.org/10.1038/s41375-021-01219-z>.

Introduction

Severe aplastic anemia (SAA) is a rare, acquired bone marrow (BM) failure disease, mediated by T cell-induced destruction of hematopoietic stem cells (HSCs) and their niche resulting in fatal pancytopenia [1, 2]. Patients diagnosed with SAA show increased levels of interferon gamma (IFN γ) in BM and peripheral blood compared to healthy individuals [3–5], and exhibit an accumulation of BM CD4 $^{+}$ T cells overexpressing IFN γ and TNF, while regulatory T cells are reduced [5]. IFN γ can induce apoptosis [3, 6, 7], limit self-renewal of HSCs, and drive HSC terminal differentiation during infection [8–10], though mechanisms of HSC loss in SAA have not been clearly defined.

Treatments for SAA patients include immunosuppressive therapies (IST; antithymocyte globulin and cyclosporine) and HSC transplantation (HSCT) [11]. The 5-year response rates with IST are ~65–70% in young patients, whereas patients over the age of 40 do not respond well. HSCT is increasingly pursued as a first-line therapy, particularly in young patients [12]. Older patients have increased rates of IST-refractory disease and have an increased risk of developing graft-versus-host disease (GvHD) in HSCT [13]. The thrombopoietin receptor agonist, eltrombopag, has shown efficacy in patients with refractory disease in combination with IST [14], however, the precise mechanisms underlying refractory disease in older patients are unclear. SAA is associated with clonal hematopoiesis and an increased risk of developing myelodysplastic disease (MDS) and leukemia [15]. As SAA and MDS exhibit altered inflammatory states [16], understanding the basic biology of SAA pathophysiology may reveal better therapeutic targets to prevent MDS in patients treated for SAA.

SAA pathogenesis is difficult to study in patients because presentation occurs with profoundly hypocellular marrow and severe cytopenias [1]. To study BMF, mouse models have been developed based on IFN γ overproduction [17], lymphocyte infusion-induced damage [18], and chemical exposure. Lymphocyte-infusion models are based on GvHD, mirror many observations in human SAA patients, and have revealed important T cell-intrinsic requirements for disease initiation [19]. In this model, macrophages (M Φ s) were required for the IFN γ -dependent loss of HSCs [20, 21]. IFN γ was necessary for persistence of M Φ s in the marrow during SAA, despite driving the loss of all other hematopoietic cells [20]. Blunting IFN γ signaling specifically in M Φ -lineage cells, or depleting M Φ s, rescued SAA. Therefore, determining mechanisms underlying the IFN γ -dependent maintenance of BM M Φ s may reveal therapeutic targets for treating SAA.

CCR5 signaling modulates inflammation during arthritis [22], infection [23–25], and colitis [26, 27]. We demonstrate that production of CCR5 ligands and increased CCR5 expression on M Φ s during SAA required IFN γ signaling in M Φ s. CCR5 antagonism rescued HSC loss, severe thrombocytopenia, and mouse death. We reveal an intrinsic requirement for CCR5 in maintaining M Φ s in the BM during SAA development, and find that even in normal aging Ccr5 expression is increased. These findings suggest CCR5 antagonism may improve SAA treatment, particularly in aged patients where CCR5 ligands are elevated [28, 29], and M Φ dysfunction promotes hematopoietic dysfunction [30].

Methods

Mice

Animal protocols were approved by the Institutional Animal Care and Use Committee (Albany Medical College). C57BL/6 (H-2^{b/b}), BALB/cAnN (H-2^{d/d}), B6/SJL (B6.SJL-*Ptprc*^q/Boy-AiTac), and FVB (FVB/NTac; H-2^{q/q}) mice were purchased (Taconic; Germantown, NY, <https://www.taconic.com/>). Macrophages-insensitive-to-IFN γ (MIIG) mice [31] were a kind gift (Dr. M. Jordan). Hybrid B6F1(H-2^{b/d}) mice were generated by crossing C57BL/6 or MIIG mice with BALB/c mice. UBC-EGFP (C57BL.6-Tg(UBG-GFP)30Scha/J), CCL5-deficient (B6.129P2-Ccl5^{tm1Hso/J}), and CCR5-deficient (B6.129P2-Ccr5^{tm1Kuz/J}) mice were purchased (Jackson Labs, Bar Harbor, Maine, <https://www.jax.org>). Aged C57BL/6J. NIA mice (20–30 months) were from National Institute on Aging. Mice were bred and housed in AMC's Animal Resource Facility under microisolator conditions. Mice were assigned to groups and given accession numbers randomly; group size was based on prior publications.

BM failure induction

Hybrid F1 mice, 6–12 weeks old, received sublethal radiation (300 RADs, ¹³⁷Cs source) followed by adoptive transfer of 60×10^6 C57BL/6 splenocytes from age- and gender-matched donors via intraperitoneal injection [6, 18, 20]. Mixed BM chimeric mice received sublethal irradiation (500 RADs) and adoptive transfer of 75×10^6 splenocytes from age- and gender-matched donor FVB mice via intraperitoneal injection. Mice were euthanized by CO₂ inhalation followed by cervical dislocation.

Mixed BM chimeras

Congenic wild-type mice (B6.SJL) were lethally irradiated via split-dose radiation (475 RADs, 24 h apart) and reconstituted with 50:50 ratio of wild-type BM (UBC-EGFP) and CCR5-deficient BM containing (10×10^6 cells total). Six weeks post reconstitution mice were screened for chimerism, and then induced to develop SAA.

Blood collection and CBCs

Blood was collected into EDTA-coated tubes and analyzed (Heska Element HT5).

Protein analysis

BM cell lysates were homogenized manually with a pestle in buffer containing IGEPAL CA-630 and proteinase inhibitors. Chemokine analysis was performed using multiplex immunoassays (Bio-Rad).

Flow cytometry

Whole BM was flushed from femurs and tibias. After RBC lysis, cell suspensions were plated and stained (antibody details in Supplementary Table 1). For IFN γ staining, cells were incubated for 2 h in monensin, prior to permeabilization (BD Pharmingen) and intracellular staining. Data were collected on an LSR II (BD Biosciences) with FACSDiva software and analyzed using FlowJo software (TreeStar, Ashland, OR).

CCL5 neutralization

Anti-CCL5 (AF478; 150 µg; R&D Systems) or isotype control antibody was diluted in PBS and administered to mice via intravenous injection on days 3, 5, and 7 postradiation. BM was harvested 12 h post final injection (8 days postradiation).

CCR5 antagonism

Maraviroc (MVC; SelleckChem) was solubilized in 100% DMSO, and diluted with Sunflower seed oil (*Helianthus annuus*, Sigma-Aldrich). Mice received daily intraperitoneal injections of MVC (30 mg/kg in 50 µl) or vehicle (Veh) starting 5 days postradiation.

Gene expression

Whole BM was flushed and pooled from hind limbs of three mice per group. RBCs were lysed and cells were stained to sort-purify MΦs (F4/80, CD11b, and CD169; BD FACSAria II) and collected in RLT Lysis Buffer (Qiagen). mRNA was isolated (Qiagen RNeasy Micro Kit) and quantitative RT-PCR (Eppendorf *realplex*² Mastercycler) performed. Transcriptional studies comparing young and aged mice and human MΦs (data sets GEO GSE100907 [30]) were utilized. MΦs were sort purified from young (2–4 months) and aged (20–30 months) mice and processed as described [30]. Human BM from young (<50 years of age) and old (>50 years of age) volunteers was obtained from healthy individuals after written consent as approved by institutional review board (University of Rochester), via BM aspiration and processed as described [30]. Differential expression analysis was performed using DESeq2–1.12.4 with an adjusted *p* value threshold of 0.05 within R version 3.3.0 [30].

Survival studies

SAA-induced and radiation control mice were monitored daily for 1 month and euthanized with when moribund. Euthanasia criteria were based on signs of dehydration, response to physical stimuli, and mobility. Mice were scored for dehydration (0: no visible tail bones and fur returns to normal after scruffing; 1: loose skin and fur while scruffing; 2: visible tail bones), stimulus response to petting or nudging (0: movement away or 1: failure to avoid stimulus), and ambulation (0: normal or 1: reduced movement, shaking, or unsteady ambulation); a combined score of 3 or more qualified for euthanasia.

Statistical analysis

Data were analyzed with GraphPad Prism software (version 9.0, La Jolla, CA) using two-tailed Student's *t* test, ANOVA and Tukey's post hoc analysis (as indicated).

Results

Chemokines in murine SAA

Pro-inflammatory cytokines can suppress hematopoiesis and are associated with SAA [32]. To investigate a potential role for chemokines in SAA, we examined blood and BM for levels of β-chemokines 8 days postradiation. Similar levels of CCL2, CCL3, and CCL4 were observed in sera from radiation controls relative to mice induced to develop SAA, though a significant increase in CCL5 was noted in SAA-induced mice (Fig. 1A). In the BM, we

observed significant increases in β -chemokines in SAA, as compared to radiation controls (Fig. 1B).

CCL5, also known as RANTES (regulated upon activation, normal T cell expressed and secreted), can be produced by a variety of cells, including Th1 cells, important drivers of SAA [33]. To test the hypothesis that T cell-derived CCL5 was an important driver of disease, we induced SAA using donor splenocytes from mice deficient in *Ccl5* (Supplementary Fig. 1A). Mice induced to develop SAA with splenocytes from CCL5-deficient mice exhibited no significant difference in time-to-death in survival studies relative to mice induced with wild-type splenocytes (Supplementary Fig. 1B), and we observed similar numbers of phenotypic HSCs ($\text{Lin}^- \text{cKit}^+ \text{CD150}^+ \text{CD48}^-$; Supplementary Fig. 1C). These data demonstrate that T cell-derived CCL5 was not necessary for disease induction. As many sources of CCL5 exist in vivo, we next neutralized CCL5 using a monoclonal antibody, administered in vivo during SAA (Fig. 1C). Blockade of CCL5 induced a subtle increase in the number of total HSCs (Fig. 1D). CD41^{hi} HSCs exhibit platelet bias, and increased CD41^{hi} HSCs were associated with protection in murine SAA [20]. Further analysis revealed that CCL5 neutralization increased CD41^{lo} HSCs, whereas CD41^{hi} HSCs were unchanged, consistent with our observation that CCL5 neutralization did not protect against SAA-induced thrombocytopenia (Fig. 1E). Together, these findings demonstrate that the chemokine CCL5 was dispensable for murine SAA disease.

Differential regulation of chemokine receptors on macrophages during SAA

CCL5 can bind multiple receptors, including CCR1, CCR3, and CCR5 [34], and CCL5–CCR5 interactions can drive $\text{M}\Phi$ survival during viral infection [35]. As $\text{M}\Phi$ persistence correlates with SAA pathogenesis [20], we next measured surface expression of chemokine receptors on $\text{M}\Phi$ s via flow cytometry (Fig. 2A, B). We noted a similar proportion of CCR1^+ $\text{M}\Phi$ s in the SAA group relative to radiation controls at both 8 and 12 days postradiation, whereas the proportion of CCR3-positive $\text{M}\Phi$ s was reduced during SAA, relative to controls (Fig. 2C). Expression of CCR5 was noted to be quite low on $\text{M}\Phi$ s in radiation controls, though it was significantly increased on $\text{M}\Phi$ s in SAA conditions on both days 8 and 12 as compared to radiation controls.

Previous studies demonstrated a requirement for $\text{IFN}\gamma$ signaling in $\text{M}\Phi$ s for SAA, as MIIG mice, where $\text{M}\Phi$ s are insensitive to $\text{IFN}\gamma$, are protected from SAA disease relative to littermate controls (LC) [20]. SAA-induced MIIG mice exhibited significantly protected BM cellularity and BM $\text{M}\Phi$ s exhibited reduced surface CCR5 relative to LC mice (Supplementary Fig. 2A–C). Furthermore, the SAA-associated increase in BM chemokines was abrogated in MIIG mice relative to LC mice with SAA (Supplementary Fig. 2D). Thus, $\text{IFN}\gamma$ -dependent pathogenesis in SAA correlated with increased chemokine production and increased $\text{M}\Phi$ -specific CCR5 expression, which may promote $\text{M}\Phi$ persistence and dysfunction in SAA-induced BM failure.

CCR5 antagonism protects against SAA pathogenesis

To determine if CCR5 signaling contributed to BM failure, SAA-induced mice were treated with the CCR5 antagonist, MVC, or Veh, beginning day 5 postradiation (Fig. 3A). MVC

is a small molecule antagonist that reversibly binds CCR5 locking the receptor in an inactive conformation. Whereas 83% of Veh-treated mice succumbed to disease beginning as early as 12 days post induction, CCR5 antagonism with MVC significantly improved survival during SAA (Fig. 3B). Cytopenias are an important clinical sign of disease, and while MVC treatment did not impact blood parameters during the 1st week of disease, MVC-treated mice exhibited increased WBCs day 12 post SAA induction, relative to Veh-treated mice (Fig. 3C). No improvement in either RBCs or hemoglobin was noted in MVC-treated mice, however, MVC induced a significant increase in circulating platelets 12 days postradiation. MVC improved overall BM cellularity 8 days post SAA induction, and the pool of hematopoietic stem and progenitors (HSPCs; Lin⁻ cKit⁺) was increased, relative to Veh-treated mice (Fig. 3D). The numbers of ST-HSCs (Lin⁻ cKit⁺ CD150⁻ CD48⁻) and LT-HSCs (Lin⁻ cKit⁺ CD150⁺ CD48⁻) were similar, but a significant increase in the number of CD41^{hi} LT-HSCs was observed in MVC-treated mice (Fig. 3E). Our observation of increased platelets and CD41^{hi} HSCs in SAA-induced mice treated with MVC parallel models of MΦ depletion [20], and suggest that platelet recovery is an important correlate of protection. Anemia was not improved at these time points, similar to studies in MIIG mice and MΦ-depletion studies [20] where protection against hematopoietic failure was not associated with a dramatic improvement in red cell parameters.

CCR5 and BM T-cell responses during SAA

MVC-treated mice showed similar overall numbers of CD90^{hi} CD3⁺ T cells on day 8, and a less striking increase in T-cell numbers was noted by day 12, relative to Veh-treated mice (Fig. 4A). The frequency of BM CD4⁺ and CD8⁺ T cells was increased in both Veh- and MVC-treated mice (Fig. 4B, C), suggesting CCR5 antagonism did not have a significant impact on BM T cell. Similar frequencies of IFNγ-secreting CD4⁺ and CD8⁺ BM T cells were observed on day 8, however, MVC treatment significantly reduced the frequency of IFNγ-secreting T lymphocytes by day 12 (Fig. 4D, E), demonstrating that MVC treatment mitigated prolonged Th1 responses in the BM.

As MVC cannot be targeted to specific cell populations, we next examined CCR5 signaling specifically in T cells by inducing SAA with splenocytes from wild-type or CCR5-deficient mice (Supplementary Fig. 3A). Similar disease outcomes were observed in mice induced with wild-type and CCR5-deficient donor splenocytes, including hypocellular BM, increased Sca1 expression, and increased BM T cells (Supplementary Fig. 3B, C). Consistent with previous findings in a model of GvHD [36], CCR5-deficient splenocytes appeared to enhance inflammation and SAA as indicated by more severe thrombocytopenia at day 8 (Supplementary Fig. 3D). These data suggest that blocking CCR5 in T cells was not sufficient for MVC-mediated protection and demonstrate that CCR5 signaling in T cells may, in fact, be protective. In line with this observation, survival studies with CCR5-deficient splenocytes revealed slightly earlier time-to-death, relative controls (Supplementary Fig. 3E). Furthermore, blocking CCR5 starting at day 8 postradiation, revealed no protection, and mice began dying at earlier time points (Supplementary Fig. 3F). Therefore, the efficacy of CCR5 antagonism may depend on timing and the distinct cellular composition in the BM during the course of disease.

CCR5 antagonism alters macrophage persistence and function in SAA

CCR5 was most highly expressed on T cells and MΦs, though MVC did not modulate expression (Supplementary Fig. 4). CCR5 expression increased slightly on monocytes and neutrophils during SAA, but MVC did not impact their frequencies or numbers in the BM (Fig. 5A, B). However, MVC treatment resulted in decreased frequencies of BM MΦs day 8 post SAA induction, but did not alter MΦ numbers, likely reflecting the overall improvement in BM cellularity with MVC treatment (Fig. 5C). MΦs and their production of TNF have been implicated in SAA pathogenesis [21], and we observed reduced TNF among MΦs in MVC-treated mice on day 12, though this was not significant (Fig. 5D). These data are consistent with transcriptional changes of sorted MΦs, where we observed an SAA-induced increase in *Tnf* and *Ccl5* expression and CCR5 antagonism abrogated this during SAA (Fig. 5E). Antagonizing CCR5 during SAA transiently reduced the frequency of MΦs, and diminished expression of two key inflammatory factors, TNF and CCL5, which may contribute to altered T-cell responses during SAA.

Macrophage-intrinsic role for CCR5 in SAA

As CCR5 can promote MΦ survival we next sought to test the hypothesis that CCR5 was required for MΦ persistence during SAA. To determine whether CCR5 was necessary specifically in MΦs we generated mixed BM chimeras containing both CCR5-deficient (CD45.2⁺; EGFP⁻) and wild-type BM (CD45.2⁺; EGFP⁺; Fig. 6A). This established an in vivo system to investigate the intrinsic role of CCR5 in MΦ persistence during SAA. SAA was induced using donor splenocytes from FVB mice [21], and mice were examined 8 days post induction. A significant decrease in HSPCs and significantly reduced platelets was observed, consistent with development of SAA (Fig. 6B, C). Among total donor BM cells, similar frequencies of WT and CCR5-deficient neutrophils and monocytes were observed in radiation control and SAA-induced mice (Fig. 6D, E). Radiation control mice exhibited similar frequencies of donor WT and CCR5-deficient MΦs, however, SAA mice exhibited significant increase in wild-type MΦs relative to CCR5-deficient cells (Fig. 6F). Together, these data demonstrate that SAA conditions, including IFN γ -producing T lymphocytes, results in CCR5 expression on MΦs and, furthermore that cell-intrinsic CCR5 expression in MΦs provides a survival advantage thus supporting their persistence in the BM (Fig. 6G).

Elevated chemokines and *Ccr5* in marrow macrophages in aging

Elevated levels of beta-chemokines have been noted in aged mice and humans [28, 29]. CCL3, CCL4, and CCL5 were significantly increased in the BM of aged mice, whereas CCL2 was diminished (Fig. 7A). Transcriptional analysis of BM MΦs showed a significant increase in *Ccl3* and *Ccl4*, and *Ccl2* and *Ccl5* were either unchanged or only moderately elevated (Fig. 7B). Among the relevant receptors for these chemokines, we observed a statistically significant increase in *Ccr5* expression among MΦs in aged mice relative to young mice (Fig. 7C). To determine the relevance of our findings to humans, we investigated expression of chemokine receptors in data sets obtained from MΦs purified from young and old volunteers [30]. Although no significant difference was observed in expression of CCR5 ligands in MΦs (data not shown), a significant increase in *Ccr5* was observed in MΦs from aged individuals (Fig. 7D). Therefore, *Ccr5* expression is increased during aging in BM

MΦs from both mice and humans, suggesting targeting CCR5 may be a novel therapeutic strategy to ameliorate SAA disease in aged patients where therapies are currently ineffective.

Discussion

Most cases of acquired SAA are idiopathic, and both genetic and environmental factors likely converge to induce disease. IFN γ has been implicated in SAA for decades, and its likely role in pathogenesis is consistent with the suppressive effects of IFN γ on hematopoiesis in a variety of contexts [10, 37, 38]. IFN γ can directly suppress HSC survival, self-renewal, and modulate differentiation [10, 39, 40], and IFN γ can also impact the function of mesenchymal stromal cells, known to support in vivo function of HSCs [41, 42]. Recently, IFN γ was found to be necessary for the survival and persistence of dysfunctional MΦs in a murine model of SAA [20]. MΦ depletion or reduction ameliorated disease in murine SAA despite having little impact on the levels of pro-inflammatory factors, including TNF and IL-1 β [20]. Here, we demonstrate a striking increase in β -chemokines in SAA, found to be dependent on IFN γ signaling in MΦs, demonstrating the local BM chemokine milieu is important for SAA initiation and/or progression.

We first focused on CCL5 as it is produced by Th1 cells, and levels were high in the marrow and blood during acute SAA. CCL5 neutralization was associated with a subtle increase in the frequency of HSCs, though this was due to increased CD41^{lo} HSCs, but not CD41^{hi} HSCs, consistent with severe thrombocytopenia in mice given CCL5-neutralizing antibodies. CCL5 may promote expansion and function of a particular subset of HSCs primed to generate platelets [20, 38, 43, 44]. Indeed, mice recovering from radiation injury benefit from infusion of recombinant CCL5, and CCR5 was necessary for hematopoietic recovery in this model [45]. A key difference between radiation injury and induction of SAA is the intensity and context of inflammatory signals. Radiation induces a moderate increase in CCL5 [45]; in contrast, SAA conditions induce a profound increase in CCL2–CCL5 in the marrow, compared to radiation alone. CCL5 is critical for megakaryopoiesis and thrombopoiesis [46], and whereas CCL5 may be important for recovery upon radiation injury, overactivation of CCR5 signaling may exhaust the hematopoietic system by driving expedited and unsustainable platelet production. CCR5 antagonism resulted in increased circulating platelets during the 2nd week of disease revealing a temporal component to the outcome of inflammatory signaling and platelet production in the context of SAA. It is also possible that receptors are differentially regulated in BM failure as compared to radiation injury.

CCL5 can be produced by a variety of cells, including activated T lymphocytes [47], however, donor T cell-derived CCL5 was not necessary for induction of SAA pathogenesis, HSC loss, and mouse death. Therefore, more potent sources of CCL5 may exist in the BM and/or redundancy with other chemokines that can bind CCR5 during SAA. We also demonstrated that CCR5-deficient T cells were able to migrate to the BM and induce disease. CCR5-deficient T cells induce severe GvHD due to failed recruitment of Tregs [48], consistent with observations of slightly more severe thrombocytopenia in SAA mice induced with CCR5-deficient splenocytes. MVC treatment beginning day 8 post-radiation did not protect against mortality, perhaps due to reduced Treg recruitment. Therefore,

additional studies are warranted to more fully understand how CCR5 antagonism impacts T lymphocytes, MΦs, and disease outcomes, when administered during disease, and, furthermore, whether later treatment can rescue established disease.

While the precise ligand(s) important for disease are not known, we reveal a specific role for CCR5 in inducing SAA. Protection afforded by treatment with the CCR5 antagonist, MVC, correlated with reduced inflammatory MΦs. Prior observations in a murine model of SAA revealed that IFN γ -dependent MΦ persistence promoted SAA pathology and HSC loss [20]. IFN γ promotes survival of MΦs during bacterial infection, via IL-6 and M-CSF [38]. Our data suggest that IFN γ may also preserve MΦs and prevent cell death by inducing expression of CCR5, as evidenced by reduced CCR5 expression on MΦs in MIIG mice, relative to LCs, during SAA that correlated with reduced numbers of MΦs in MIIG mice [20, 38]. Our findings are consistent with observations that CCR5 promotes MΦ survival during viral infection [35]. By generating an in vivo setting where both CCR5-positive and CCR5-deficient cells were present, we were able to show that CCR5 signaling was necessary to maintain MΦs in the BM in SAA conditions. It will be important to determine if this is unique to acute, inflammatory diseases or if it is also relevant to low-level chronic inflammation, such as that observed in aging.

How MΦs promote hematopoietic failure and HSC loss is still unclear, however, the ability of MΦs to interact with many different cell types and produce a variety of inflammatory factors likely contributes to microenvironmental changes that drive hematopoietic dysfunction. Interestingly, only very mild rescue of anemia was observed with MVC, whereas thrombocytopenia was profoundly improved. Previous studies where MΦs were transiently depleted also failed to improve anemia, but rescued hematopoietic function, consistent with the observation that MΦs support erythropoiesis. While MVC treatment does not improve acute anemia, it is possible that anemia improves over time due to improved mouse survival and rescued HSCs.

Viral infections, including parvovirus B19, cytomegalovirus (CMV), and Epstein–Barr virus (EBV), have been associated with SAA [1, 49]. Parvovirus can infect a variety of cells and mediate direct cytotoxic effects [50, 51]. CMV and EBV are typically acquired in childhood and remain latent in immune cells, and their reactivation can occur upon IST in patients with SAA [52]. EBV and CMV elicit production of chemokines and expression of chemokine receptors, and the CCL5–CCR5 axis plays essential role(s) in T-cell expansion and migration during infection in vivo [53–55]. CMV and EBV infections are often subclinical, and their presence in the right context may promote signals necessary for SAA development. Our studies suggest the possibility that viral infection triggers a chemokine signaling axis, further supporting CCR5 in initiation of SAA.

CCR5 is a co-receptor for HIV and a mutant allele of *Ccr5* (Δ32 allele) provides natural resistance to HIV infection. MVC is currently approved for patients with CCR5-tropic HIV, and in HIV-infected patients where therapies were failing, MVC resulted in improved control of virus, and a significant improvement in WBCs, platelet numbers, and hemoglobin [56]. CCR5 antagonism was not only beneficial as an antiviral, but also improved hematopoietic function. CCR5 antagonists have also been pursued to reduce

tumor-associated MΦs and regulatory T cells [57, 58]. Blocking CCR5 signaling in an F₁ mouse model of GvHD reduced T-cell infiltration into the liver, mitigated liver injury, and reduced FasL mRNA levels in the liver [59]. MVC has been studied as part of the standard GvHD prophylaxis following HSC transplant where it reduced the incidence of GvHD in high-risk patients 6 months post HSC transplant [60]. In mouse models of GvHD, CCR5 signaling can also prevent disease by controlling migration of regulatory T cells [36, 48], thus mechanisms regulating migration and function of BM T cells, particularly during SAA, warrant further investigation.

Treatment for SAA has made remarkable advancements in recent years, however, refractory disease is devastating to individual patients and their families, and older patients continue to have poor outcomes [1]. Antagonizing CCR5 may augment IST and/or HSCT, particularly in aged patients as expression of *Ccr5* in MΦs is increased relative to young counterparts. Older patients may exhibit refractoriness to standard IST and exhibit more GvHD in part due to heightened responsiveness to chemokines. Although we did not observe an increase in chemokines expressed by MΦs from aged humans, other sources of these ligands exist in the BM that may impact MΦs locally. Additional studies are warranted to decipher how signaling via CCR5 in MΦs, and other cell types, impacts blood production in disease and aging.

Supplementary Material

Refer to Web version on PubMed Central for supplementary material.

Acknowledgements

The authors would like to thank Angelica Costello and Hui Jin Jo for technical assistance. This work was supported by a Aplastic Anemia and MDS International Foundation grant to KCM, BM160071 and BM190079 (DOD-BMFRP-IDA) to KCM and R01 AG046293 to LMC.

References

1. Young NS. Aplastic anemia. *N Engl J Med*. 2018;379:1643–56. [PubMed: 30354958]
2. Chen J, Brandt JS, Ellison FM, Calado RT, Young NS. Defective stromal cell function in a mouse model of infusion-induced bone marrow failure. *Exp Hematol*. 2005;33:901–8. [PubMed: 16038782]
3. Dufour C, Corcione A, Svahn J, Haupt R, Battilana N, Pistoia V. Interferon gamma and tumour necrosis factor alpha are overexpressed in bone marrow T lymphocytes from paediatric patients with aplastic anaemia. *Br J Haematol*. 2001;115:1023–31. [PubMed: 11843845]
4. Sloand E, Kim S, Maciejewski JP, Tisdale J, Follmann D, Young NS. Intracellular interferon-gamma in circulating and marrow T cells detected by flow cytometry and the response to immunosuppressive therapy in patients with aplastic anemia. *Blood*. 2002;100:1185–91. [PubMed: 12149196]
5. Nistico A, Young NS. Gamma-interferon gene expression in the bone marrow of patients with aplastic anemia. *Ann Intern Med*. 1994;120:463–9. [PubMed: 8311369]
6. Chen J, Lipovsky K, Ellison FM, Calado RT, Young NS. Bystander destruction of hematopoietic progenitor and stem cells in a mouse model of infusion-induced bone marrow failure. *Blood*. 2004;104:1671–8. [PubMed: 15166031]
7. Chen J, Feng X, Desierto MJ, Keyvanfar K, Young NS. IFN-gamma-mediated hematopoietic cell destruction in murine models of immune-mediated bone marrow failure. *Blood*. 2015;126: 2621–31. [PubMed: 26491068]

8. Morales-Mantilla DE, King KY. The role of interferon-gamma in hematopoietic stem cell development, homeostasis, and disease. *Curr Stem Cell Rep.* 2018;4:264–71. [PubMed: 30148048]
9. Zombos NC, Djeu JY, Young NS. Interferon is the suppressor of hematopoiesis generated by stimulated lymphocytes in vitro. *J Immunol.* 1984;133:769–74. [PubMed: 6203978]
10. de Bruin AM, Demirel O, Hooibrink B, Brandts CH, Nolte MA. Interferon-gamma impairs proliferation of hematopoietic stem cells in mice. *Blood.* 2013;121:3578–85. [PubMed: 23487025]
11. Marsh JC, Ball SE, Cavenagh J, Darbyshire P, Dokal I, Gordon-Smith EC, et al. Guidelines for the diagnosis and management of aplastic anaemia. *Br J Haematol.* 2009;147:43–70. [PubMed: 19673883]
12. Gupta V, Eapen M, Brazauskas R, Carreras J, Aljurf M, Gale RP, et al. Impact of age on outcomes after bone marrow transplantation for acquired aplastic anemia using HLA-matched sibling donors. *Haematologica.* 2010;95:2119–25. [PubMed: 20851870]
13. Ghimire S, Weber D, Mavin E, Wang XN, Dickinson AM, Holler E. Pathophysiology of GvHD and other HSCT-related major complications. *Front Immunol.* 2017;8:79. [PubMed: 28373870]
14. Winkler T, Fan X, Cooper J, Desmond R, Young DJ, Townsley DM, et al. Treatment optimization and genomic outcomes in refractory severe aplastic anemia treated with eltrombopag. *Blood.* 2019;133:2575–85. [PubMed: 30992268]
15. Sun L, Babushok DV. Secondary myelodysplastic syndrome and leukemia in acquired aplastic anemia and paroxysmal nocturnal hemoglobinuria. *Blood.* 2020;136:36–49. [PubMed: 32430502]
16. Barreyro L, Chlon TM, Starczynowski DT. Chronic immune response dysregulation in MDS pathogenesis. *Blood.* 2018;132: 1553–60. [PubMed: 30104218]
17. Lin FC, Karwan M, Saleh B, Hodge DL, Chan T, Boelte KC, et al. IFN-gamma causes aplastic anemia by altering hematopoietic stem/progenitor cell composition and disrupting lineage differentiation. *Blood.* 2014;124:3699–708. [PubMed: 25342713]
18. Bloom ML, Wolk AG, Simon-Stoos KL, Bard JS, Chen J, Young NS. A mouse model of lymphocyte infusion-induced bone marrow failure. *Exp Hematol.* 2004;32:1163–72. [PubMed: 15588941]
19. Roderick JE, Gonzalez-Perez G, Kuksin CA, Dongre A, Roberts ER, Srinivasan J, et al. Therapeutic targeting of NOTCH signaling ameliorates immune-mediated bone marrow failure of aplastic anemia. *J Exp Med.* 2013;210:1311–29. [PubMed: 23733784]
20. McCabe A, Smith JNP, Costello A, Maloney J, Katikaneni D, MacNamara KC. Hematopoietic stem cell loss and hematopoietic failure in severe aplastic anemia is driven by macrophages and aberrant podoplanin expression. *Haematologica.* 2018;103: 1451–61. [PubMed: 29773597]
21. Sun W, Wu Z, Lin Z, Hollinger M, Chen J, Feng X, et al. Macrophage TNF-alpha licenses donor T cells in murine bone marrow failure and can be implicated in human aplastic anemia. *Blood.* 2018;132:2730–43. [PubMed: 30361263]
22. Lan YY, Wang YQ, Liu Y. CCR5 silencing reduces inflammatory response, inhibits viability, and promotes apoptosis of synovial cells in rat models of rheumatoid arthritis through the MAPK signaling pathway. *J Cell Physiol.* 2019;234:18748–62. [PubMed: 31066041]
23. Hardison JL, Wrightsman RA, Carpenter PM, Kuziel WA, Lane TE, Manning JE. The CC chemokine receptor 5 is important in control of parasite replication and acute cardiac inflammation following infection with *Trypanosoma cruzi*. *Infect Immun.* 2006;74:135–43. [PubMed: 16368966]
24. Carr DJ, Ash J, Lane TE, Kuziel WA. Abnormal immune response of CCR5-deficient mice to ocular infection with herpes simplex virus type 1. *J Gen Virol.* 2006;87:489–99. [PubMed: 16476970]
25. Kroetz DN, Deepe GS Jr. An aberrant thymus in CCR5^{-/-} mice is coupled with an enhanced adaptive immune response in fungal infection. *J Immunol.* 2011;186:5949–55. [PubMed: 21478401]
26. Mencarelli A, Cipriani S, Francisci D, Santucci L, Baldelli F, Distrutti E, et al. Highly specific blockade of CCR5 inhibits leukocyte trafficking and reduces mucosal inflammation in murine colitis. *Sci Rep.* 2016;6:30802. [PubMed: 27492684]

27. Matsuzaki K, Hokari R, Kato S, Tsuzuki Y, Tanaka H, Kurihara C, et al. Differential expression of CCR5 and CRTH2 on infiltrated cells in colonic mucosa of patients with ulcerative colitis. *J Gastroenterol Hepatol.* 2003;18:1081–8. [PubMed: 12911667]
28. Mo R, Chen J, Han Y, Bueno-Cannizares C, Misesk DE, Lescure PA, et al. T cell chemokine receptor expression in aging. *J Immunol.* 2003;170:895–904. [PubMed: 12517955]
29. Ergen AV, Boles NC, Goodell MA. Rantes/Ccl5 influences hematopoietic stem cell subtypes and causes myeloid skewing. *Blood.* 2012;119:2500–9. [PubMed: 22289892]
30. Frisch BJ, Hoffman CM, Latchney SE, LaMere MW, Myers J, Ashton J, et al. Aged marrow macrophages expand platelet-biased hematopoietic stem cells via Interleukin1B. *JCI Insight.* 2019;4:e124213.
31. Lykens JE, Terrell CE, Zoller EE, Divanovic S, Trompette A, Karp CL, et al. Mice with a selective impairment of IFN-gamma signaling in macrophage lineage cells demonstrate the critical role of IFN-gamma-activated macrophages for the control of protozoan parasitic infections in vivo. *J Immunol.* 2010;184:877–85. [PubMed: 20018611]
32. Dufour C, Corcione A, Svahn J, Haupt R, Poggi V, Beka'ssy AN, et al. TNF-alpha and IFN-gamma are overexpressed in the bone marrow of Fanconi anemia patients and TNF-alpha suppresses erythropoiesis in vitro. *Blood.* 2003;102:2053–9. [PubMed: 12750172]
33. Solomou EE, Keyvanfar K, Young NS. T-bet, a Th1 transcription factor, is up-regulated in T cells from patients with aplastic anemia. *Blood.* 2006;107:3983–91. [PubMed: 16434488]
34. Pakianathan DR, Kuta EG, Artis DR, Skelton NJ, Hebert CA. Distinct but overlapping epitopes for the interaction of a CC-chemokine with CCR1, CCR3 and CCR5. *Biochemistry.* 1997;36:9642–8. [PubMed: 9289016]
35. Tyner JW, Uchida O, Kajiwarra N, Kim EY, Patel AC, O'Sullivan MP, et al. CCL5-CCR5 interaction provides antiapoptotic signals for macrophage survival during viral infection. *Nat Med.* 2005;11:1180–7. [PubMed: 16208318]
36. Welniak LA, Wang Z, Sun K, Kuziel W, Anver MR, Blazar BR, et al. An absence of CCR5 on donor cells results in acceleration of acute graft-vs-host disease. *Exp Hematol.* 2004;32:318–24. [PubMed: 15003318]
37. Baldridge MT, King KY, Boles NC, Weksberg DC, Goodell MA. Quiescent haematopoietic stem cells are activated by IFN-gamma in response to chronic infection. *Nature.* 2010;465:793–7. [PubMed: 20535209]
38. McCabe A, Zhang Y, Thai V, Jones M, Jordan MB, MacNamara KC. Macrophage-lineage cells negatively regulate the hematopoietic stem cell pool in response to interferon gamma at steady state and during infection. *Stem Cells.* 2015;33:2294–305. [PubMed: 25880153]
39. Selleri C, Maciejewski JP, Sato T, Young NS. Interferon-gamma constitutively expressed in the stromal microenvironment of human marrow cultures mediates potent hematopoietic inhibition. *Blood.* 1996;87:4149–57. [PubMed: 8639773]
40. Matatall KA, Shen CC, Challen GA, King KY. Type II interferon promotes differentiation of myeloid-biased hematopoietic stem cells. *Stem Cells.* 2014;32:3023–30. [PubMed: 25078851]
41. Schurch CM, Riether C, Ochsenbein AF. Cytotoxic CD8(+) T cells stimulate hematopoietic progenitors by promoting cytokine release from bone marrow mesenchymal stromal cells. *Cell Stem Cell.* 2014;; 14:460–72. [PubMed: 24561082]
42. Goedhart M, Cornelissen AS, Kuijk C, Geerman S, Kleijer M, van Buul JD, et al. Interferon-gamma impairs maintenance and alters hematopoietic support of bone marrow mesenchymal stromal cells. *Stem Cells Dev.* 2018;27:579–89. [PubMed: 29649408]
43. Haas S, Hansson J, Klimmeck D, Loeffler D, Velten L, Uckelmann H, et al. Inflammation-induced emergency megakaryopoiesis driven by hematopoietic stem cell-like megakaryocyte progenitors. *Cell Stem Cell.* 2015;17:422–34. [PubMed: 26299573]
44. Gekas C, Graf T. CD41 expression marks myeloid-biased adult hematopoietic stem cells and increases with age. *Blood.* 2013;121: 4463–72. [PubMed: 23564910]
45. Piryani SO, Kam AYW, Vu UT, Chao NJ, Doan PL. CCR5 signaling promotes murine and human hematopoietic regeneration following ionizing radiation. *Stem Cell Rep.* 2019; 13:76–90.

46. Machlus KR, Johnson KE, Kulenthirarajan R, Forward JA, Tippy MD, Soussou TS, et al. CCL5 derived from platelets increases megakaryocyte proplatelet formation. *Blood*. 2016;127:921–6. [PubMed: 26647394]
47. Song A, Chen YF, Thamatrakoln K, Storm TA, Krensky AM. RFLAT-1: a new zinc finger transcription factor that activates RANTES gene expression in T lymphocytes. *Immunity*. 1999;10:93–103. [PubMed: 10023774]
48. Wysocki CA, Jiang Q, Panoskaltsis-Mortari A, Taylor PA, McKinnon KP, Su L, et al. Critical role for CCR5 in the function of donor CD4+ CD25+ regulatory T cells during acute graft-versus-host disease. *Blood*. 2005;106:3300–7. [PubMed: 16002422]
49. Young NS, Bacigalupo A, Marsh JC. Aplastic anemia: pathophysiology and treatment. *Biol Blood Marrow Transplant*. 2010;16:S119–125. [PubMed: 19782144]
50. Young NS, Brown KE. Parvovirus B19. *N Engl J Med*. 2004;350:586–97. [PubMed: 14762186]
51. Chisaka H, Morita E, Yaegashi N, Sugamura K. Parvovirus B19 and the pathogenesis of anaemia. *Rev Med Virol*. 2003;13: 347–59. [PubMed: 14625883]
52. Scheinberg P, Fischer SH, Li L, Nunez O, Wu CO, Sloand EM, et al. Distinct EBV and CMV reactivation patterns following antibody-based immunosuppressive regimens in patients with severe aplastic anemia. *Blood*. 2007;109:3219–24. [PubMed: 17148582]
53. Prod'homme V, Tomasec P, Cunningham C, Lemberg MK, Stanton RJ, McSharry BP, et al. Human cytomegalovirus UL40 signal peptide regulates cell surface expression of the NK cell ligands HLA-E and gpUL18. *J Immunol*. 2012;188: 2794–804. [PubMed: 22345649]
54. McSharry BP, Avdic S, Slobedman B. Human cytomegalovirus encoded homologs of cytokines, chemokines and their receptors: roles in immunomodulation. *Viruses*. 2012;4:2448–70. [PubMed: 23202490]
55. Ma W, Feng L, Zhang S, Zhang H, Zhang X, Qi X, et al. Induction of chemokine (C-C motif) ligand 5 by Epstein-Barr virus infection enhances tumor angiogenesis in nasopharyngeal carcinoma. *Cancer Sci*. 2018;109:1710–22. [PubMed: 29569795]
56. Nozza S, Galli L, Bigoloni A, Gianotti N, Spagnuolo V, Carbone A, et al. Four-year outcome of a PI and NRTI-sparing salvage regimen: maraviroc, raltegravir, etravirine. *N Microbiol*. 2014;37: 145–51.
57. Lin S, Sun L, Lyu X, Ai X, Du D, Su N, et al. Lactate-activated macrophages induced aerobic glycolysis and epithelial-mesenchymal transition in breast cancer by regulation of CCL5-CCR5 axis: a positive metabolic feedback loop. *Oncotarget*. 2017;8:110426–43. [PubMed: 29299159]
58. Halvorsen EC, Hamilton MJ, Young A, Wadsworth BJ, LePard NE, Lee HN, et al. Maraviroc decreases CCL8-mediated migration of CCR5(+) regulatory T cells and reduces metastatic tumor growth in the lungs. *Oncoimmunology*. 2016;5:e1150398. [PubMed: 27471618]
59. Murai M, Yoneyama H, Harada A, Yi Z, Vestergaard C, Guo B, et al. Active participation of CCR5(+)/CD8(+) T lymphocytes in the pathogenesis of liver injury in graft-versus-host disease. *J Clin Invest*. 1999;104:49–57. [PubMed: 10393698]
60. Reshef R, Luger SM, Hexner EO, Loren AW, Frey NV, Nasta SD, et al. Blockade of lymphocyte chemotaxis in visceral graft-versus-host disease. *N Engl J Med*. 2012;367:135–45. [PubMed: 22784116]

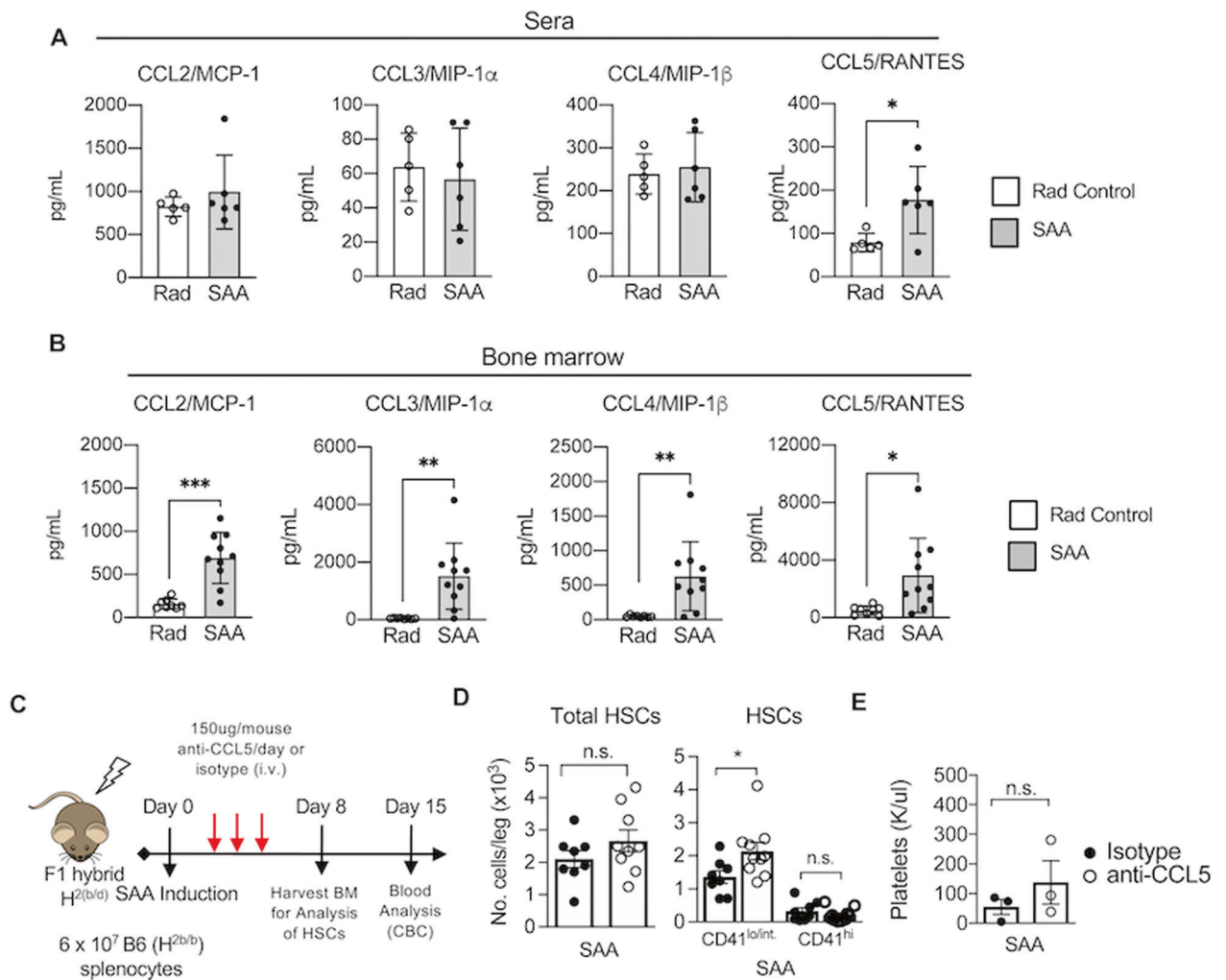


Fig. 1. Increased chemokines in the BM during SAA in mice.

Mice were induced to develop SAA via splenocyte transfer following sublethal irradiation. Sera (**A**) isolated from peripheral blood and total bone marrow homogenates (**B**) were evaluated for beta-chemokine concentrations via a Luminex assay for radiation control mice (open circle, open bar) and SAA-induced mice (closed circle, grey bar) 8 days postirradiation; $n = 5-6$ per group. C Mice were induced to develop SAA and treated with a neutralizing antibody to CCL5 (clone number 53405.111, R&D systems) on days 5-7 via intravenous administration. D BM was evaluated on day 8 post splenocyte transfer and LT-HSCs (LSK, CD150⁺ CD48⁻) and CD41^{+/lo} and CD41^{hi} LT-HSCs were enumerated in BM in SAA mice treated with isotype (filled circle) or anti-CCL5 antibodies (open circles). E Circulating platelets were evaluated at 15 days post SAA induction in mice treated with Isotype or anti-CCL5 antibodies as described in panel (C). Data represent data pooled from two independent experiments, mean \pm SD is shown, and significance was determined by a Student's *t* test; * $p < 0.05$, ** $p < 0.01$, *** $p < 0.001$.

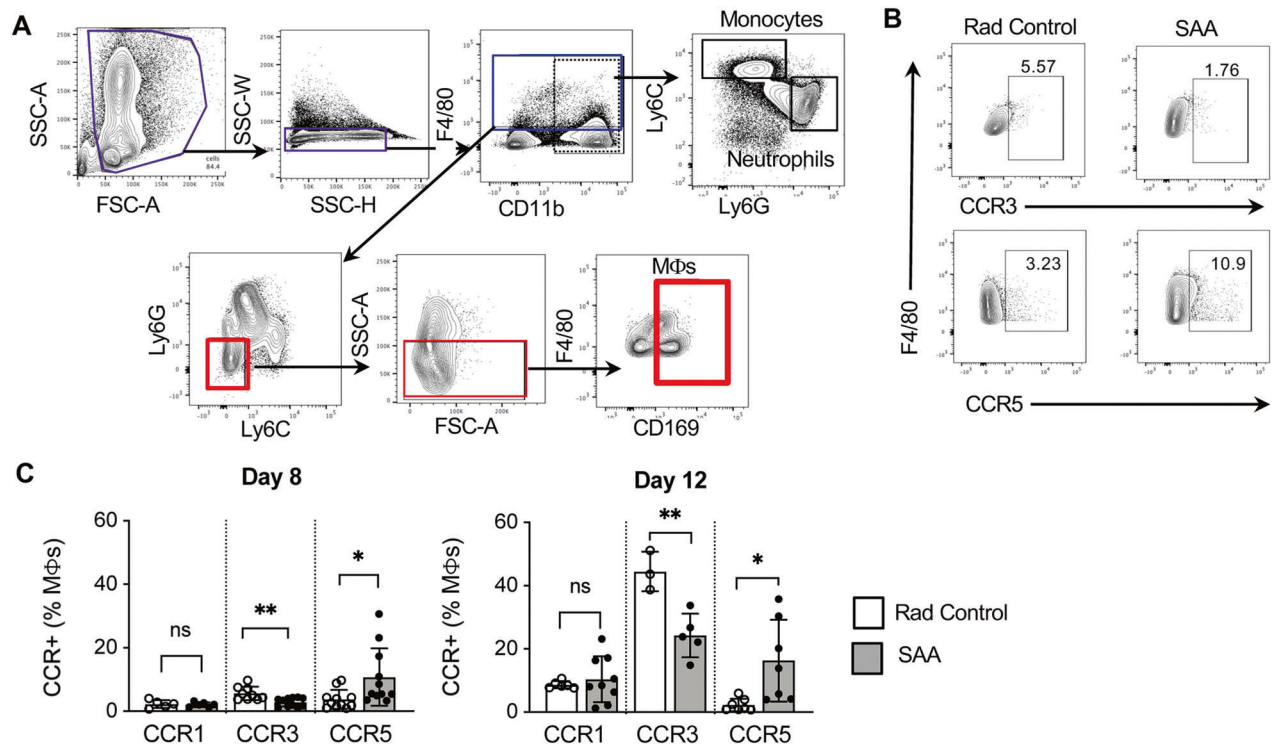


Fig. 2. CCR5 expression is increased on macrophages during SAA.

Mice were induced to develop SAA and BM was examined 8 and 12 days post-radiation.

A The gating strategy to identify myeloid populations via flow cytometry is shown and populations were analyzed as follows: monocytes (CD11b⁺ Ly6C^{hi} Ly6G⁻), neutrophils (CD11b⁺ Ly6C^{int} Ly6G^{hi}), and macrophages (MΦs) (F4/80⁺ Ly6C⁻ Ly6G⁻ SSC-A^{low} CD169⁺). **B** Flow cytometry plots representing CCR3 and CCR5 gating strategy for F4/80⁺ Ly6C⁻ Ly6G⁻ SSC-A^{low} CD169⁺ MΦs day 12 post-radiation. **C** The percent of CCR1, CCR3, and CCR5-positive MΦs was determined via flow cytometry on days 8 (left panel) and 12 (right panel) post-radiation for rad control (open) and SAA-induced mice (gray filled). The mean ± SD is shown and data are pooled from two independent experiments, $n = 3-11$ per group; significance was determined by a Student's t test. * $p < 0.05$, ** $p < 0.01$.

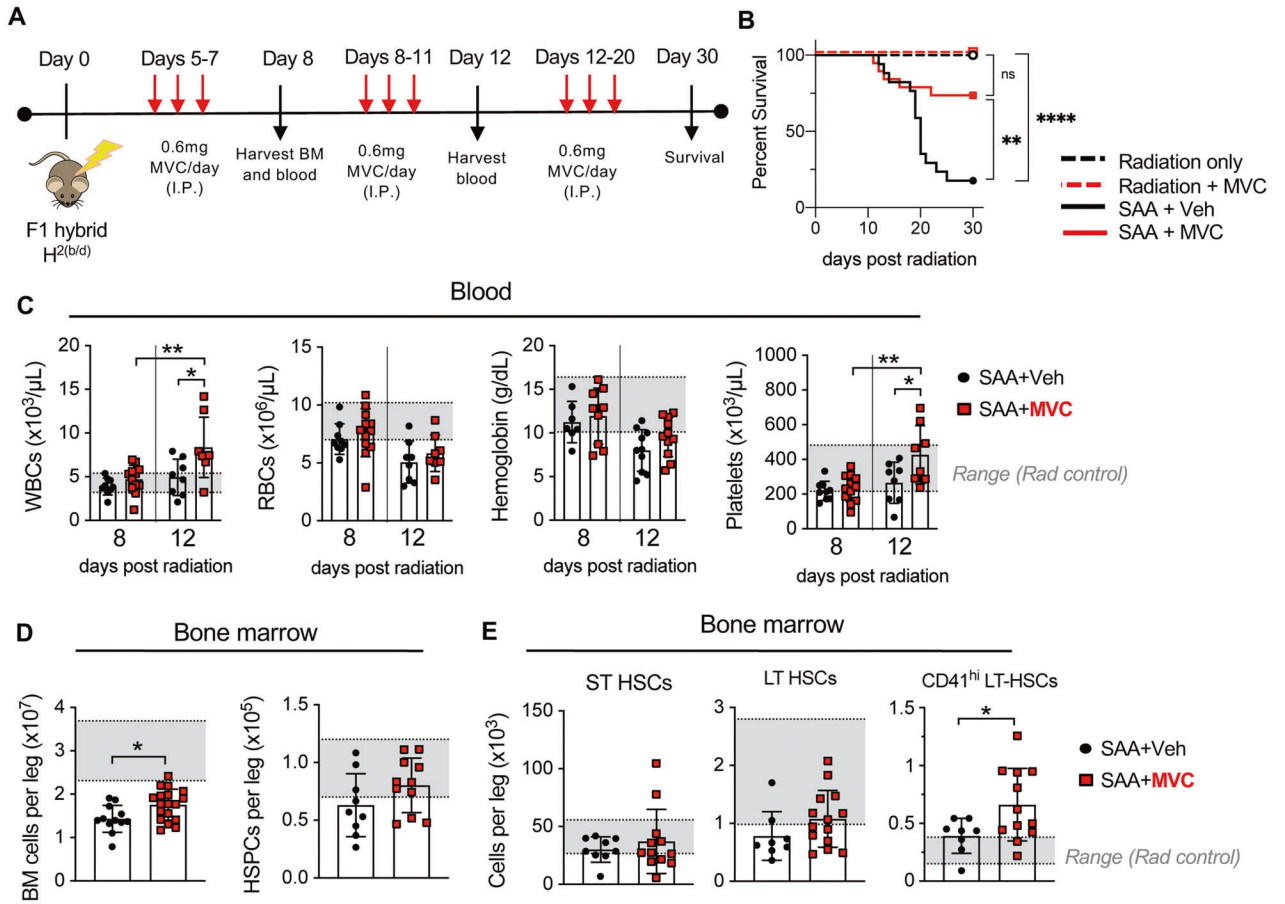


Fig. 3. CCR5 antagonism with maraviroc improves survival and bone marrow cellularity when administered during SAA.

A F₁ hybrid mice were induced via splenocyte transfer following sublethal irradiation and treated with 0.6 mg maraviroc (MVC) via i.p. injection beginning 5 days postirradiation; **B** Percent survival 30 days postirradiation; radiation only (black dashed line) $n = 9$; radiation control mice treated with MVC (red dashed line) $n = 9$; SAA mice treated with vehicle (black solid line) $n = 17$; SAA mice treated with MVC (red solid line) $n = 19$. Data pooled from two individual experiments. Significance determined by log-rank (Mantel-Cox) test; * $p < 0.05$, ** $p < 0.01$, **** $p < 0.0001$. **C** Complete blood counts for white blood cells (WBCs), red blood cells (RBCs), hemoglobin, and platelets are shown for Veh-treated mice (closed circles) and MVC-treated mice (red squares) on days 8 and 12 postirradiation and ranges for radiation controls are depicted in gray (filled area, y-axis). **D** Total bone marrow cellularity and number of HSPCs per leg for Veh-treated mice (closed circles) and MVC-treated mice (red squares). **E** Graphs depict absolute number of short-term HSCs (ST-HSCs) ($Lin^- cKit^+ CD150^- CD48^-$), long-term HSCs (LT-HSCs) ($Lin^- cKit^+ CD150^{hi} CD48^-$), and $CD41^{hi}$ LT-HSCs, respectively. Data pooled from two individual experiments per time point showing mean \pm SD, $n = 5-12$. Significance between groups within each time point was determined by a Student's t test. * $p < 0.05$, ** $p < 0.01$.

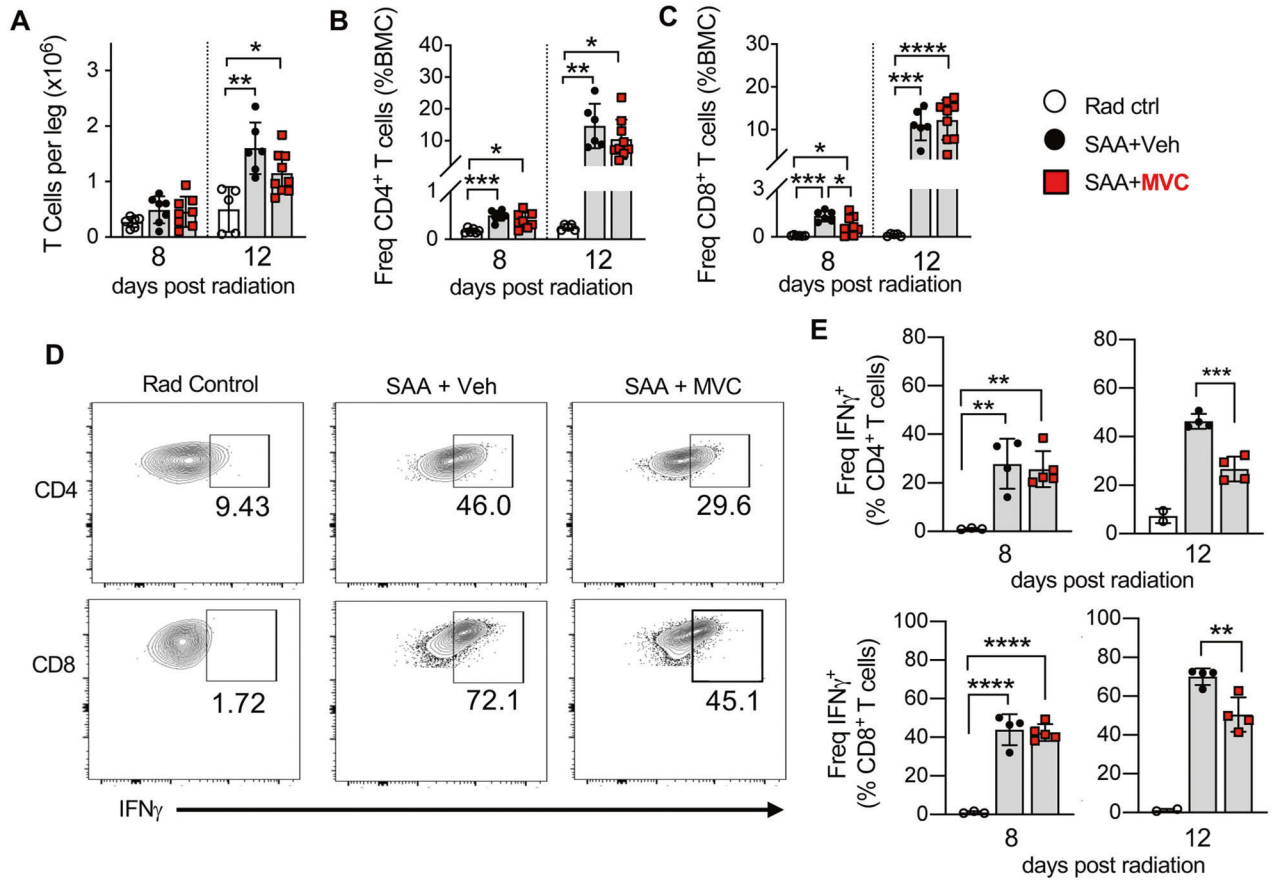


Fig. 4. The impact of CCR5 antagonism on T lymphocytes in SAA pathogenesis.

F1 hybrid mice were induced via splenocyte transfer following sublethal irradiation and treated with 0.6 mg MVC via i.p. injection beginning 5 days post-radiation. BM was harvested 8 and 12 days post-radiation. **A** Absolute number of BM T cells (CD90^{hi} CD3⁺); frequencies of CD4⁺ (**B**) and CD8⁺ (**C**) subsets are shown as percent of total BM cells (%BMC). Data pooled from two individual experiments per time point, $n = 5-9$ per group per time point; statistical significance for all data was determined by ANOVA followed by Tukey's post hoc analysis for multiple comparisons. * $p < 0.05$, ** $p < 0.01$, *** $p < 0.001$, **** $p < 0.0001$. **D** Flow cytometry plots representing gating strategy for IFN γ expressing CD4⁺ and CD8⁺ T cells; numbers on plots represent the percent of cells within the gated region. **E** Frequencies of IFN γ expressing CD4⁺ and CD8⁺ T cells 8 and 12 days post-radiation. Data show one experiment, $n = 2-5$ per group per time point, showing the mean \pm S.D. Statistical significance for day 8 data was determined by ANOVA followed by Tukey's post hoc analysis for multiple comparisons. * $p < 0.05$, ** $p < 0.01$, *** $p < 0.001$, **** $p < 0.0001$. Statistical significance for day 12 data was determined by a Student's t test. ** $p < 0.01$, *** $p < 0.001$.

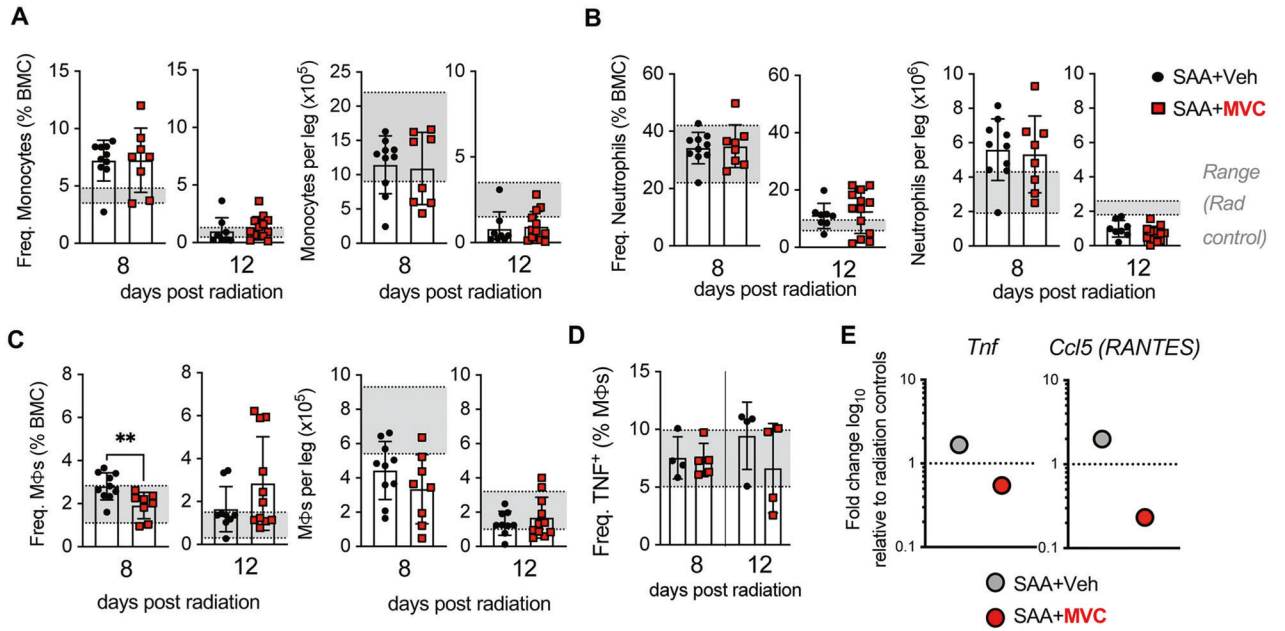


Fig. 5. CCR5 antagonism alters macrophage numbers and function during SAA.

F₁ hybrid mice were induced via splenocyte transfer following sublethal irradiation and treated with 0.6 mg MVC via i.p. injection beginning 5 days postradiation. BM was harvested 8 and 12 days postradiation and myeloid cells were analyzed in SAA mice treated with either vehicle (closed circles) or MVC (red squares) with ranges for radiation controls shown by gray fill (y-axis). **A** Frequency and absolute number of monocytes per leg. **B** Frequency and absolute number of neutrophils per leg. **C** Absolute number of MΦs per leg. **D** Intracellular staining of TNF was performed and the frequency of TNF expressing MΦs is shown. Data pooled from two individual experiments showing mean \pm S.D., $n = 6-12$. Significance between groups was determined by a Student's *t* test. $*p < 0.05$. **E** Bone marrow was pooled from three individual mice per group for fluorescence-based cell sorting. mRNA was extracted from MΦs (F4/80⁺ CD11b⁺ Gr-1⁻ CD169⁺ SSC-A^{low}) for qRT-PCR analysis. MΦ gene expression is normalized to glyceraldehyde 3-phosphate dehydrogenase (GAPDH) and relative to radiation controls. Each qRT-PCR was performed at least twice and data points represent the mean of replicates. Data for *Tnf* are two individual pooled experiments and for *Ccl5* are a representative experiment from individual experiments showing similar trends.

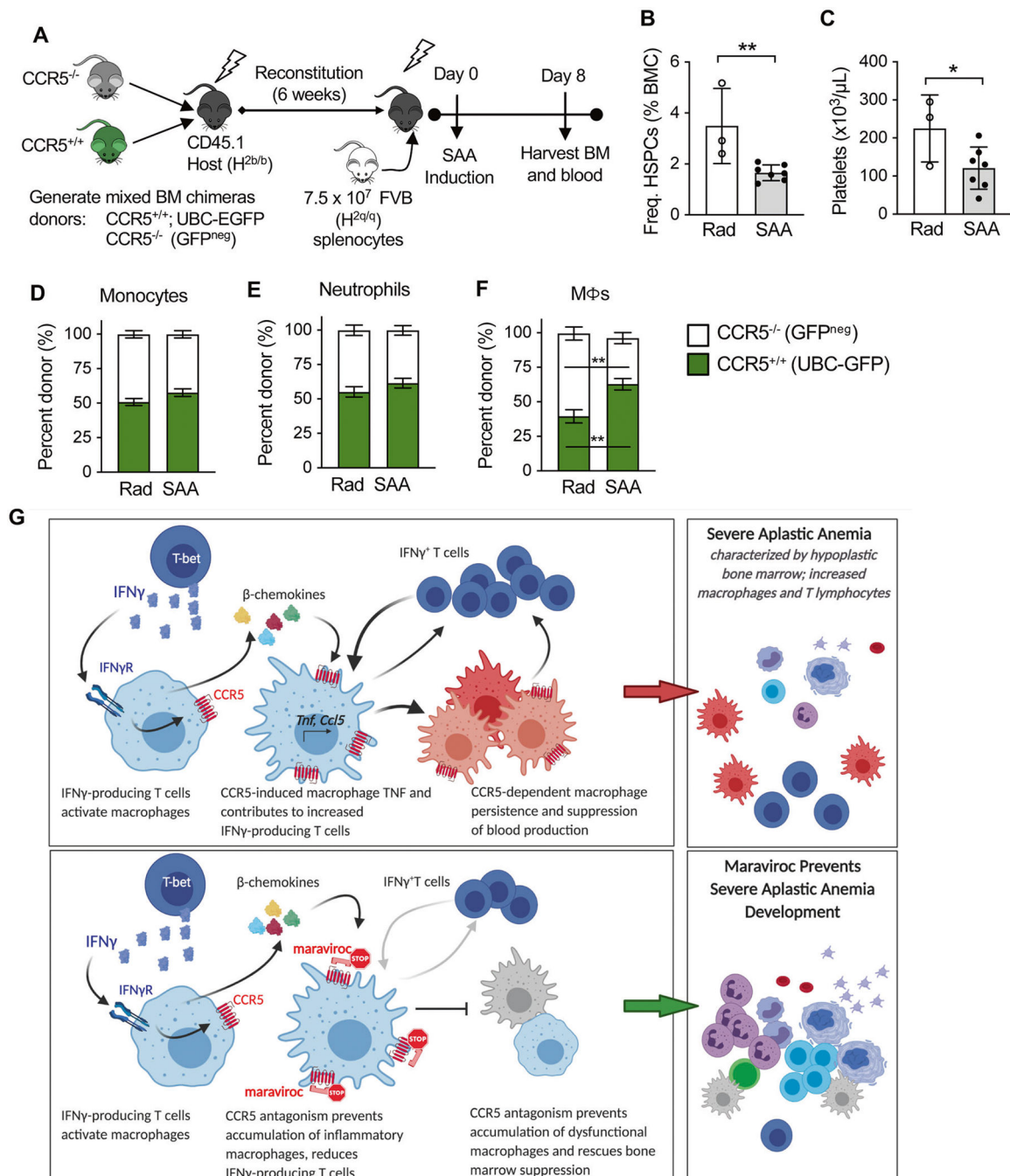


Fig. 6. Intrinsic role for CCR5 in macrophages in SAA.

A Mixed BM chimeric mice were generated by lethally irradiating CD45.1 mice (split dose of 950 RADs total) followed by transplant of a mixture of CCR5^{-/-} and wild-type whole BM (total 10×10^6 cells total). Following reconstitution of the hematopoietic system, mice were either sublethally irradiated (500 RADs) (open bars) or induced to develop SAA (grey bars) via sublethal irradiation plus adoptive transfer of splenocytes (75 million cells) from FVB donors. **B** BM was analyzed by flow cytometry and the frequency of HSPCs (Lin⁻ cKit⁺ (LK)) among total BM cells (BMCs) is shown for radiation controls

(Rad; open bars) and SAA mice (gray bars); $n = 3-7$ per group. **C** Platelets as determined by CBC are shown in Rad (open bars) and SAA mice (gray bars). Significance between groups was determined by a Student's t test. $*p < 0.05$, $**p < 0.01$. The percent donor wild type (UBG-GFP, green filled) or CCR5 deficient (open) among total bone marrow cells in radiation control mice (Rad; open bars, $n = 3$) and SAA mice (filled bars; $n = 7$) is shown for the indicated populations: **D** monocytes ($CD11b^+ Ly6C^{hi} Ly6G^{lo}$), **E** neutrophils ($CD11b^+ Ly6C^{lo} Ly6G^{hi}$), or **F** MΦs ($F4/80^+ Ly6C^- Ly6G^- SSC-A^{low} CD169^+$). Statistical significance was determined using a two-way ANOVA, $**p < 0.01$, and data are representative of two independent experiments showing the mean \pm S.D. **G** Schematic model illustrating the roles of CCR5 during development of SAA. $IFN\gamma$ signaling in MΦs promotes β -chemokine expression in the BM and increased expression of CCR5 on MΦs. Signaling through CCR5 enhances the Th1 responses and increased $IFN\gamma$ -producing T cells, promotes persistence of inflammatory MΦs, and results in hematopoietic failure. Antagonism of CCR5 alters MΦ function and reduces the $IFN\gamma$ -producing T cells, thus preventing hematopoietic failure.

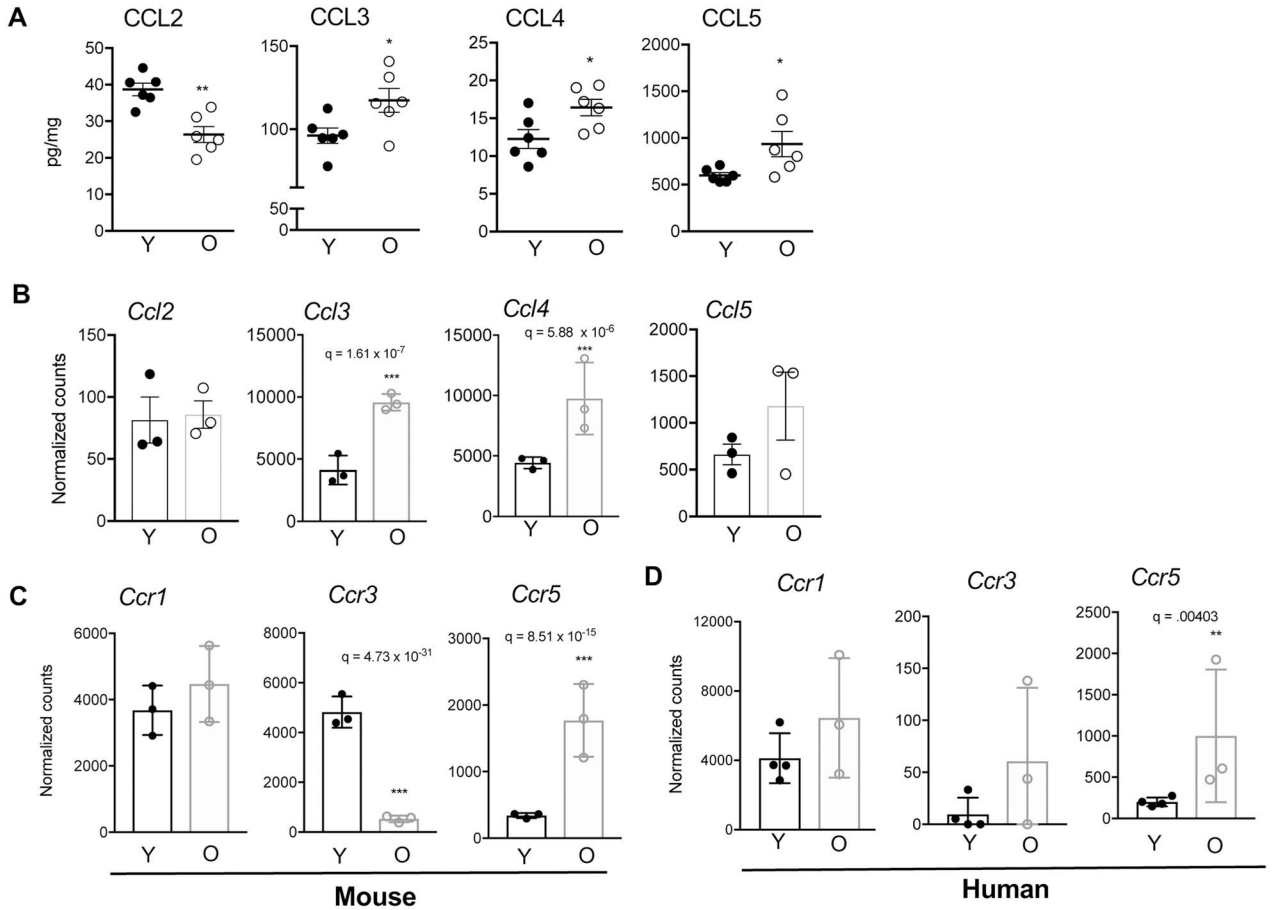


Fig. 7. Chemokines and their receptors in aged mice and humans.

A Total bone marrow protein was evaluated for beta-chemokines in marrow from young mice (8–10 weeks of age; filled circles) and aged mice (15–18 months of age; open circles). Concentrations of the indicated chemokine were normalized to total protein and each dot represents a single mouse, $n = 6$ per group and error bars represent SEM. Significance between groups was determined by a Student's t test. $*p < 0.05$, $**p < 0.01$. **B** Expression of chemokines in sorted MΦs from young and aged mice ($n = 3$ mice per group). **C** Expression of chemokine receptors in sorted MΦs from young and aged mice ($n = 3$ mice per group). **D** Expression of chemokine receptors in sorted MΦs from young volunteers ($n = 4$; <50 years of age) and aged volunteers ($n = 3$; >50 years of age). Differential expression analysis was performed using DESeq2–1.12.4 with an adjusted p value (q , exact value shown) within R version 3.3.0.